Journal of Solid State Chemistry 303 (2021) 122519

Contents lists available at ScienceDirect

Journal of Solid State Chemistry

journal homepage: www.elsevier.com/locate/jssc

Solid-state photoswitching in arylazopyrazole-embedded polydimethylsiloxane composite thin films

Kesete Ghebreyessus [a,*], Ikemefuna Uba [b], Demetris Geddis [b], Uwe Hömmerich [c]

[a] Department of Chemistry and Biochemistry, Hampton University, Hampton, VA, 23668, USA
[b] Department of Electrical and Computer Engineering and Hampton University, Hampton, VA, 23668, USA
[c] Department of Physics, Hampton University, Hampton, VA, 23668, USA

ARTICLE INFO

Keywords:
Solid-state photoswitching
Arylazopyrazole
Photoresponsive composite thin films
Photoactuator

ABSTRACT

Arylazopyrazoles (AAPs) show significant potential as a new family of molecular photoswitches owing to their efficient reversible trans -to- cis photoisomerization behavior and the high thermal stability of their metastable cis -isomer. In this study, AAPs have been used for the fabrication of solid-state photoswitchable polydimethylsiloxane (PDMS) based composite thin films. The thin films were prepared by using PDMS as a polymer matrix and different concentrations of AAPs as chromophores at 150 °C via spin-coating. The photoswitching behavior of the AAPPDMS composite films and the pristine AAP samples induced by irradiation with specific wavelength of light were investigated. We found that the as prepared AAPPDMS composite films showed rapid and near-quantitative (>98%) reversible trans -to- cis isomerization upon alternating irradiation with UV (λ = 365 nm) and green (λ = 525 nm) light which is comparable to the isomerization behavior of the pristine AAP chromophores in solution. This indicates that the excellent photoswitching property of the AAPs is preserved in the solid-state of the AAP-PDMS composite films. The results also show that the optical properties of the AAP-PDMS composite films can be tuned by using different ratios of the AAP chromophores and exposure to UV-light irradiation. Additionally, the thin films were tested for their photo-actuation behavior by UV–vis spectroscopy. Irradiation of the thin film with alternating 365 nm UV and 525 nm green light lead to a slight reversible bending behavior. This is presumably caused by the light-induced conformational change of the AAP moiety embedded within the PDMS matrix and the soft nature of the PDMS. This methodology provides a new approach for exploring the fabrication of polymers with enhanced mechanical behavior and solidstate photoswitching properties. Arylazopyrazoles (AAPs) show significant potential as a new family of molecular photoswitches owing to their efficient reversible trans -tocis photoisomerization behavior and the high thermal stability of their metastable cis - isomer. In this study, AAPs have been used for the fabrication of solid-state photoswitchable polydimethylsiloxane (PDMS) based composite thin films. The thin films were prepared by using PDMS as a polymer matrix and different concentrations of AAPs as chromophores at 150 °C via spin-coating. The photoswitching behavior of the AAP-PDMS composite films and the pristine AAP samples induced by irradiation with specific wavelength of light were investigated. We found that the as prepared AAP-PDMS composite films showed rapid and near-quantitative (>98%) reversible trans -to- cis isomerization upon alternating irradiation with UV (λ = 365 nm) and green (λ= 525 nm) light which is comparable to the isomerization behavior of the pristine AAP chromophores in solution. This indicates that the excellent photoswitching property of the AAPs is preserved in the solid-state of the AAP-PDMS composite films. The results also show that the optical properties of the AAP-PDMS composite films can be tuned by using different ratios of the AAP chromophores and exposure to UV-light irradiation. Additionally, the thin films were tested for their photo-actuation behavior by UV–vis spectroscopy. Irradiation of the thin film with alternating 365 nm UV and 525 nm green light lead to a slight reversible bending behavior. This is presumably caused by the light-induced conformational change of the AAP moiety embedded within the PDMS matrix and the soft nature of the PDMS. This methodology provides a new approach for exploring the fabrication of polymers with enhanced mechanical behavior and solid-state photoswitching properties.

* Corresponding author. Department of chemistry and Biochemistry, Hampton University Hampton, 200 William R Harvey Way, VA, 23668, USA.
E-mail address: Kesete.Ghebreyessus@hamptonu.edu (K. Ghebreyessus).

https://doi.org/10.1016/j.jssc.2021.122519
Received 3 July 2021; Received in revised form 14 August 2021; Accepted 16 August 2021

1. Introduction

Photoswitchable molecules that undergo reversible conformational change between two distinct isomers upon irradiation with light continue to attract considerable attention. Nowadays, particular attention has been focused on their potential applications in molecular actuators [1–3], optical memory devices [4,5], solar energy storage materials [6,7], photoresponsive surfaces [8–11] and drug delivery vesicles [12–15]. Among the various types of photoswitchable molecules studied, azobenzenes have been widely investigated due to the facile synthetic access and the option to modify the substitution pattern to fine tune and improve the photochemical properties [16–19]. The photoinduced isomerization of azobenzenes results in a *cis*-isomer with a shorter length scale. The resulting conformational change is accompanied by pronounced modification of the chemical and physical properties of the azo photoswitch.

As an alternative approach, optimization of the photoswitching performance of azobenzene has been inspired by the investigation of azoheteroarenes. In particular, arylazopyrazoles (AAPs) have been recently introduced as improved light-responsive molecular switches compared to their azobenzene counterpart [20–29]. These heterocyclic azo compounds represent an emerging new class of photoswitches with redshifted wavelength, long thermal half-lives, facile synthetic access and near quantitative reversible *trans*-to-*cis* isomerization upon irradiation with UV or green light, respectively. Substitution of one of the benzene rings from the conventional azobenzene class with a five membered hetero-aromatic ring leads to a large separation of the π-π* and n-π* absorbance of the molecules to enable optimized photochromic behavior. This large separation enables the selective isomerization of both isomers with high efficiency to complete *cis*-to-*trans* photo-conversion. Owing to these favorable features application of AAPs is emerging in various optically addressable materials that include supramolecular gels [22–24], surfactants [25–27], host-guest systems [22, 28–30], coordination chemistry [23,34], photopharmacology and DNA nanotechnology [30–33]. The light-induced isomerization in this type of photo-switchable molecules is often accompanied by a large conformational change which necessitates a large degree of conformational freedom. As a consequence, majority of the functional properties of AAPs have been investigated in solution or soft molecular assemblies such as gels and liquid crystals [20–24,34], which greatly limits the scope of their potential applications. Hence, exploring a general methodology allowing for reversible isomerization of these photochromic substances within solid-state materials would be highly desirable. However, despite the rapidly growing interest in azo-heterocycles, studies on their photoswitching properties in the solid-sate have been scarcely explored.

In this study, we decide to explore the light-induced solid-state isomerization of AAPs by simply doping the photochromic compounds into polydimethylsiloxane (PDMS) matrix without directly anchoring to the polymer backbone. The doping method avoids the cumbersome and multiple-step reactions involved in synthesizing complex copolymers. The choice of PDMS as a host material is motivated by its excellent thermal and optical properties, chemical inertness and amenable processing [35–45]. It is a low cost flexible and optically transparent polymer that is inert to many organic and inorganic compounds [35–45]. Owing to its unique properties, it has been extensively used as a template for nano/microscale patterning and as a substrate for microfluidic channel formation [38–43]. In recent years, PDMS polymers embedded with photochromic materials have also been fabricated with the aim of formulating unique transparent and flexible photoswitchable sensor systems [42–44]. Most of the reported photoswitching PDMS systems in the literature are based on the photochromic spiropyran [42,43] and to a lesser extent azobenzene [44]. Although the study of PDMS composites embedded with photochromic substances is an emerging combination for various applications, the construction of PDMS composites having photoswitchable AAPs molecular switches has not been described yet.

Furthermore, alongside with the design and preparation of hybrid organic-polymer composite films, organic-inorganic oxide composites having both the advantages of inorganic oxides and the film forming property and flexibility of organic polymers, and possess high hardness and high temperature resistance have been widely explored [46–48]. In addition, composite films based on purely all inorganic oxides have also been extensively studied [49–60]. T***hese hybrid composite materials are prepared by using various methods that include sol-gel technology, blending method, and molecular self-assembly among others*** [49–60]. Compared with organic polymeric systems, the optical properties of oxide based materials can be greatly improved due to the high degree of control over both composition and nanostructure that can be achieved by mixing virtually any ratios to produce the hybrid materials. This in turn allows for fine tuning of structure-property relationships leading to a broad range of applications in the fields of magnetism, optics and nanotechnology [48–60]. It should also be noted that organic-inorganic composite thin films based on inorganic oxides doped with the photo-responsive azobenzene moiety that display light-induced photo--isomerization and optical switching characteristics have been recently reported [48].

Herein, the fabrication of a photoswitchable AAP doped PDMS composite films, which combine the unique properties of AAPs and PDMS is reported. W***hile there are numerous methods such as electro-deposition, chemical vapor deposition, physical vapor deposition and sol-gel dip-coating method that can be applied to prepared oxide and organic-inorganic composite films, the hybrid thin films described in this study are prepared via spin-coating method*** [48,51–56, 61–63]. Fig. 1 shows the chemical structure of the AAPs used in this study. The solid-state optical properties of the AAP-PDMS composite films were investigated by UV–vis spectroscopy. The results show that the light-induced reversible *trans*-to-*cis* photoswitching behavior of the AAPs was preserved in the solid-state within the AAP- PDMS matrix. Additionally, the films show a slight light-induced bending actuation caused by the conformational change due to the isomerization of the AAP moiety embedded with the PDMS matrix.

2. Experimental

2.1. Materials and methods

All reactions were carried out under nitrogen atmosphere. All chemicals and solvents used of the synthesis of the AAP photoswitches and preparation of the AAP-PDMS composite films were purchased from commercial sources and used as received. N-methylhydrazine, polydimethylsiloxane (PDMS), 1-bromo-6-hexanol, ethyl acetate, Na_2SO_4, K_2CO_3, acetone, potassium iodide, 4-aminophenol, 2,4-pentanedione and dichloromethane were purchased from Sigma Aldrich and were used without further purification.

2.2. Synthesis of 3-(1,3,5-trimethyl-4-(phenoldiazenyl)-pyrazol-1-yl)-hexanol (AAP1)

The precursor compounds 3-((2-4-hydroxyphenylhydazono))-pentane-2,4-dione (**2**), 4-((1,3,5-Trimethyl-1H-pyrazol-4-yl)diazenyl))-phenol (**3**) and 3-(3,5-dimethyl-4-(phenyldiazenyl)-pyrazol-1-yl)-propionic acid (AAP2) were prepared according to literature and methods described in our recent work [20–22,64,65].

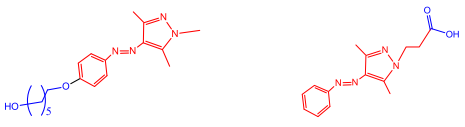

AAP1 AAP2

Fig. 1. Chemical structure of the arylazopyrazole photoswitches AAP1 and AAP2.

To a solution of the intermediated compound 4-((1,3,5-Trimethyl-1H-pyrazol-4-yl)diazenyl))-phenol (**3**) (0.53 g, 2.23 mmol) in acetonitrile (50 mL), K_2CO_3 (1.43 g, 10.4 mmol), KI (21.5 mg, 0.13 mmol) was added dropwise to 1-bromo-6-hexanol (1.27 g, 7.0 mmol), then it was stirred and allowed to reflux at 80 °C for 6 h. After completion of the reaction, the solvent was evaporated under reduced pressure yielding an orange solid. The residue was washed with water. Then, it was dissolved in ethyl acetate and dried over Na_2SO_4. The solvent was removed under reduced pressure affording yellow-orange solid product of AAP1 (Scheme 1).

Yellow solid; yield: 90% (AAP1): ^{1}H-NMR (400 MHz, $CDCl_3$): δ: 8.01 (d, $J = 8.8$ Hz, 2H), 7.35 (d, $J = 8.9$ Hz, 2H), 4.04 (t, $J = 6.4$ Hz, 2H), 3.96 (s, 3H), 3.65 (q, $J = 6.4$ Hz, 2H), 2.25 (quint, $J = 6.5$ Hz, 2H), 1.90 (quint, $J = 7.2$ Hz, 2H), 1.65-1.58 (m, 4H). ^{13}C-NMR (100 MHz), $CDCl_3$) δ: 162.1 (1C), 154.4 (1C), 146.8 (1C), 135.5 (2C), 127.2 (1C), 124.1 (1C), 114.5 (2C), 67.9 (1C), 62.8 (1C), 39.6 (1C), 33.8 (1C), 29.2 (1C), 25.8 (1C), 24.8 (1c), 14.1 (1C), 9.7 (1C). Anal. Calculated for [$C_{18}H_{26}N_4O_2$]: C, 65.47; H, 7.87; N, 16.96. Found: C, 65.29; H, 7.80; N, 19.56.

2.3. Preparation of the arylazopyrazole PDMS (AAP-PDMS) films

Preparation of the arylazopyrazole incorporated PDMS films (AAP-PDMS) was carried out using the commercially available Sylgard 184 silicone elastomer kit from Dow Inc. following procedures previously reported for analogous spiropyran or azobenzene photochromes [42–44]. While there are many methods (e.g., electrodeposition, chemical vapor deposition, physical vapor deposition, sol-gel dip-coating method) available for preparing hybrid organic-inorganic oxide or organic-polymer composite materials, the composite films described in this study are prepared via spin-coating [48, 51–56, 61–63]. First, different molar solutions (0.03 M, 0.02 M, 0.015 M) of the AAP1 and AAP2 photoswitches were prepared by dissolving 0.10 g of the AAPs molecules in 10 mL of acetone at room temperature. Then, 20 g of the PDMS precursor of the Sylgard 184 silicone elastomer kit was mixed with the curing agent in a weight ratio of 10:1. Next, 1.0 mL of the acetone solutions (0.020 M or 0.015 M) of the AAP photochromes were poured into the PDMS elastomer mixture and stirred well for 2 min to ensure thorough mixing. The clear homogeneous gel formed using 0.02 M or 0.015 M solutions was then spin-coated at a high speed of 1000 rpm on 75 × 25 mm glass slide pre-cleaned with acetone to give a 25 μm thick film. Similarly, the sample containing 0.030 M solution was spin-coated at a slow speed of 200 rpm to give a dense film of 127 μm thickness. The resulting coated glass slides are then heated on a hot plate at 150 °C for 22 min to yield a clear uniform yellow colored AAP-doped PDMS thin films. The resulting film was of uniform composition and without vagaries associated with repeated fabrication. The dense film (127 μm) was designed with the aim to study the effect of concentration of the photochromic substance and thickness on the isomerization process.

2.4. Photoswitching studies of AAP-PDMS thin films

The successful integration of the photochromic arylazopyrazole moiety into the PDMS film was ascertained by UV–vis spectroscopy. A strip of the hardened AAP-PDMS film was peeled off from the glass substrate and adhered to a film-sample holder of the spectrophotometer fitted to conduct photoisomerization studies in solid-state samples. For the *trans*-to-*cis* isomerization, the UV–vis irradiation was carried out by placing the AAP-PDMS film in the sample-holder and exposed to 365 nm light from a hand-held lamp. Subsequent irradiation with green light of 525 nm was used for the reverse *cis*-to-*trans* photoisomerization studies. The spectrum of undoped PDMS of the same thickness was used as baseline to ensure that measured spectrum was entirely that of the photoswitch.

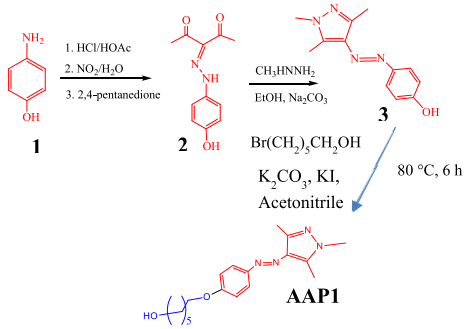

Scheme 1. Synthetic route for **AAP1.**

2.5. Photoswitching stability

To probe for the reproducibility and the stability, the reversible *trans*-to-*cis* and *cis*-to-*trans* isomerization was examined using a 25 μm film repeated over four cycles. Initially, absorbance of the film was measured, then the film was irradiated with 365 nm UV for 5 min to attain *cis*-state and subsequently irradiated with 525 nm green light successively for 5 min followed by measurement of the corresponding absorbance.

2.6. Characterization methods

^{1}H and ^{13}C NMR spectra of the samples were recorded on a JEOL Eclipse2-400 MHz spectrometer using solvent resonances as internal references relative to TMS. Solution state UV–visible absorption spectra were recorded on a Varian Cary 60 BIO spectrometer from Agilent technologies. Photoisomerization was induced by irradiating solutions of the molecular switches in a quartz cuvette at room temperature with UV light at 365 nm, followed immediately by recording the absorption spectrum. Dry acetone, acetonitrile or dichloromethane (DCM) solvents were used for all UV–visible measurements. The extent of isomerization at the photostationary state is estimated based on the following difference equation:

$$\%\ \mathrm{Cis} = \frac{A_{trans} - A_{Cis}}{A_{trans}} \times 100$$

Where A_{trans} is the absorbance for the *trans* isomer at λ_{max} before light irradiation and A_{cis} is the absorbance for the *cis* isomer at the same wavelength measured at the photostationary state [66–68]. The reverse *cis*-to-trans isomerization was conducted by irradiating using green light ($\lambda = 525$ nm).

In the solid-state, photoisomerization properties of the AAP1 and AAP2 doped PDMS composite films were probed using a Shimadzu 600 UV–Vis spectrophotometer by recording absorbance spectra following each irradiation time interval. Two light sources were used for photoswitching: hand held UV-light ($\lambda = 365$ nm) for *trans*-to-*cis* isomerization and high-power LED ($\lambda = 525$ nm) for *cis*-to-*trans* isomerization at different time intervals. SEM images were recorded with a JEOL 6390, operating with an acceleration voltage of 5 kV. The pressure inside the chamber was kept constant below 10^{-5} mbar and the working distance was set to 39 mm.

3. Results & discussion

3.1. Synthesis of molecular switches

Carboxyl and hydroxyl group functionalized AAPs were synthesized follow literature procedures [20–22,46,47] and methods developed in our laboratory [23,34] (Scheme 2) with the aim to fabricate AAP doped PDMS composite films and matrix and explore the solid-state photoswitching behavior (for details of the synthesis procedures and characterization see experimental part). The AAP1 photoswitch has been characterized by ^{1}H NMR, ^{13}C NMR, and UV–vis spectroscopy. Similar to previously reported AAP based photoswitches, the presence of the

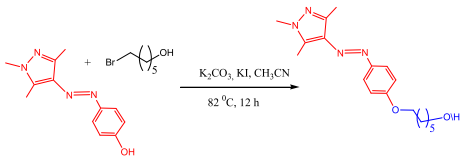

Scheme 2. Synthetic Route for AAP1.

characteristic peaks of the CH_3 group of the pyrazole moieties in the 2.50–2.60 ppm range in the NMR spectra indicates that, in all cases, the molecular switches exist in their more stable trans isomers under normal conditions [20, 23, 34, 64].

3.2. Preparation of the AAP-PDMS composite films

The AAP photoswitches were incorporated into the PDMS Sylgard 184 elastomer following procedures previously reported for analogous spiropyran or azobenzene.

photochromes [42–44]. The amount of the AAP switches in the PDMS composite film was kept at a lower concentration to avoid oversaturation of the UV–vis measurements. The obtained transparent uniform yellow AAP embedded PDMS composite film (AAP-PDMS) was cut into strips for subsequent UV–vis studies (Fig. 2a and b).

3.3. Photoisomerization studies of AAP1 and AAP2 in solution

UV–vis spectroscopy was carried out to study the photoisomerization properties of the AAPs molecular switches in solution for comparison purposes to the solid-state AAP-PDMS composite films. The UV–vis spectra and photoisomerization studies of AAP2 was described in our recent studies [23]. Absorption spectra of AAP1 in acetone (2.0×10^{-5} M) is shown in Fig. 3. Similar to AAP2, under normal conditions, the AAP1 photoswitche existed in the stable *trans*-isomer form. Before UV-light irradiation at $\lambda = 365$ nm, the *trans*-isomer of AAP1 displayed two characteristic absorption bands at ($\lambda = 345$ nm) and a weak band at 440 nm (Fig. 3a). Analogous to reported literature studies on arylazopyrazoles [20–23], the intense absorption band for the *trans*-isomer was assigned to the π-π* transitions, whereas the broad, weak band at around 440 nm was assigned to the n-π* transitions. Upon irradiation with UV light (λ =365 nm) for 0–2 min, the *trans*-form was easily converted to the *cis*-

isomer (Fig. 4). This was clearly shown by a significant decrease in the π-π* transition at 345 nm and an increase in the n-π* 440 nm (Fig. 3a), which were indicative of the formation of the *cis*-isomer. The *trans*-to-*cis* isomerization of AAP1 reached a photostationary state (PSS) within 2 min. Further irradiation of the sample solution beyond 2 min did not give any

significant changes in the spectral features. The *cis*-to-*trans* ratio at the PSS was found to be.

94:6 for compound AAP1, as estimated from the UV–vis spectra using the equation described in the literature [67,68]. In this calculation, it is assumed that before light irradiation, the absorption band at 345 nm is a

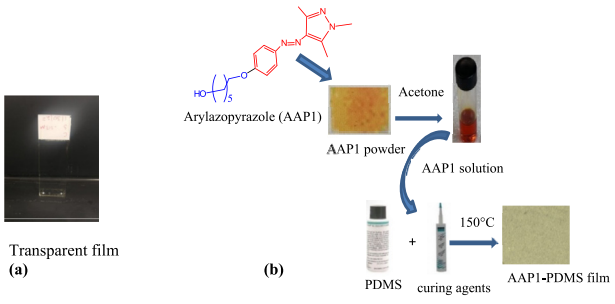

Fig. 2. Preparation process for the AAP1-PDMS composite films.

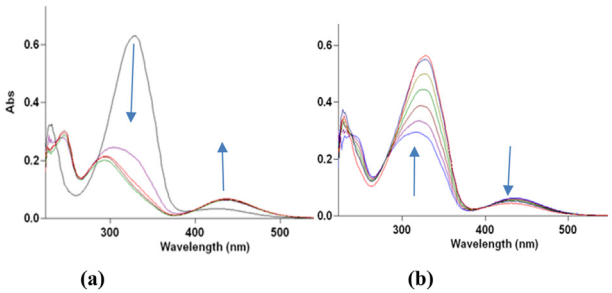

Fig. 3. UV–Vis absorbance spectral changes of the pristine AAP1 in acetone (2×10^{-5} M); **(a)** *trans*-to-*cis* isomerization after irradiation for different times from 0 to 2 min at $\lambda = 365$ nm; **(b)** Spectra of irradiated solution of compound AAP1 (*cis*-to-*trans* isomerization) upon irradiation with $\lambda = 530$ nm and recorded after different times of irradiation from 5 to 20 min.

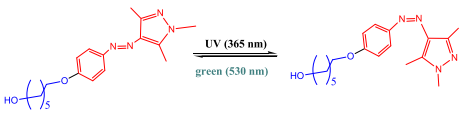

Fig. 4. Reversible photoisomerization of the **AAP1** molecule.

100% from the *trans*-state [67,68].

The reverse *cis*-to-*trans* photo-isomerization of AAP1 was also studied by UV–vis spectroscopy. For example, upon exposure of a solution of AAP1 to UV light ($\lambda = 365$ nm) for 2 min, and then irradiating the sample with green ($\lambda = 530$ nm) for 15 min led to the near full recovery of the original absorption spectrum of the *trans*-isomer (Fig. 3b). The *trans*-to-*cis* ratio was found to be 90:10.

3.4. UV–vis behavior of the AAP-PDMS composite films

After curing the sample at 150 °C for 22 min, analysis of the UV–vis spectra of the AAP-PDMS composite films were carried out in a manner similar to those of the solution based samples. Initially, to assess the photophysical properties of the samples in the solid-state, the UV–vis spectra was examined using the thick 127 μm AAP1-PDMS composite film as a function of time (Fig. 5). Encouragingly, as shown in Fig. 5, upon irradiation with UV light (λ =365 nm) the *trans*-isomer of the AAP1 embedded in the PDMS matrix is converted into the metastable *cis*-configuration, which is evidenced by a decrease in the intensity of the π-π* peak at 340 nm and an increase in the n-π* band at 450 nm. The PSS

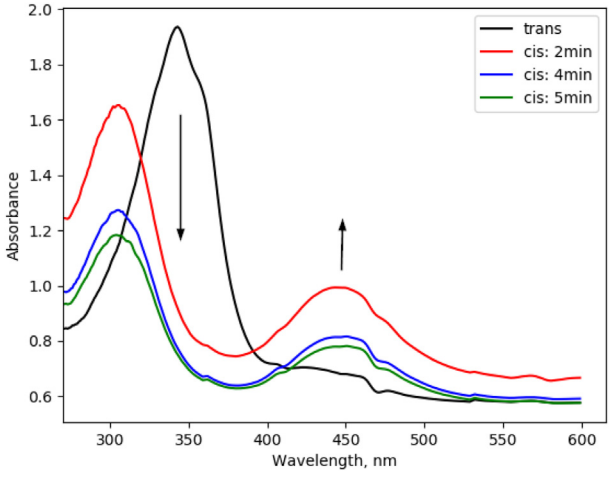

Fig. 5. UV–vis absorbance spectral changes of the 125 μm thickness of the AAP1-PDMS composite film for the *trans*-to-*cis*-isomerization upon irradiation for different times from 0 to 5 min at $\lambda = 365$ nm.

state at the 340 nm band is achieved after 5 min of irradiation. At the PSS the *trans*-to-*cis* ratio was found to be 39:61 as estimated from the UV–vis spectra using the equation described in the literature [67,68]. Similar to the solution based samples, in this calculation, it is assumed that before light irradiation, the absorption at 340 nm is a 100% from the *trans*-state [67,68]. The photoisomerization of AAP1 induces a change in the molecular size. When incorporated into the PDMS polymer matrix, there is a certain free volume requirement for photoisomerization of the AAP1 photoswitch to occur. Hence, the reduced isomerization efficiency of the AAP1 photoswitch embedded in the thick (127 μm) PDMS matrix could be attributed to the steric hindrance impeding the desired light-induced conformational change due to the high concentration of the AAP1 in the composite film.

To further assess the efficiency of the photoisomerization, the UV–vis absorption spectra of the AAP1-PDMS composite was investigated using a thin (25 μm) film (Fig. 6a). The composite film was prepared by spin-coating of 0.020 M solution of the AAP1 into the PDMS matrix. The absorbance spectra before UV light irradiation clearly shows that the composite films investigated are dominated by the *trans*-state at room temperature (Fig. 6a). However, upon continuous irradiation with 365 nm UV light for 5 min the *trans*-isomer is transformed to the *cis*-state which is manifested by a decrease of the absorption peak centered at 340 nm and a slight increase in the peak around 450 nm. Afterward, irradiation with 525 nm green light for 5 min results in an increase of the absorption peak at 340 nm and decrease in the peak at 450 nm indicating the reverse switching of the *cis*-isomer to the *trans*-isomer (Fig. 6b). Thus, irradiation of the sample with green light for 5 min resulted in the retrieval of the original spectrum with a slightly higher intensity of the peak at the 340 nm, indicating that a small percentage of the *cis*-form of the AAP1 was present in the of the original sample. Further irradiation of the composite film beyond 5 min did not give any significant changes.

in the spectral features. Clearly, these changes in the absorbance spectra are indicative of the conformation changes due to the *trans*-to-*cis* photoisomerization of the AAP1 embedded in the PDMS matrix. These results indicate that the AAP1 compound embedded in the PDMS matrix exhibited a quantitative (~ 100) reversible photoswitching efficiency in the solid-state (Fig. 6b). The high switching efficiency of the AAP1 in the thin (25 μm) film of the PDMS matrix could be attributed to its longer chain that gave rise to a larger volume change in response to light irradiation.

The optical switching and performances of the composite film doped with 0.020 M of the photochromic arylazopyrazole moiety was studied by irradiating with alternating UV light 365 nm and green light 525 nm for four cycles at room temperature (Fig. 6c). During this process the composite film was irradiated with UV light for 5 min followed by the immediate measuring of the UV–vis absorbance spectrum of the film. Subsequently, the composite film was irradiated with green light for 5 min, then the UV–vis absorption spectrum of the film was immediately measured again. Four such cycles were measured repeatedly, at the 340 nm absorption wavelength and each UV–vis absorption spectrum was carefully recorded resulting in the characteristic optical switching behavior shown in Fig. 6c. The results in Fig. 6c show that there are several periods of reversible photo-isomerization upon exposure to alternating UV and green lights, indicating a good optical switching performance and strong fatigue resistance.

In summary, these significant changes in the absorption spectra of the samples are indicative of the efficient reversible photoisomerization of the AAP moiety embedded in the alternating irradiation with 365 nm UV light (5 min) and 525 green light (5 min). This process appears to be fully reversible for at least four cycles without photodegradation, as we didn't observe any change in the peak absorbance between cycles (Fig. 6c). The profound differences in photo-isomerization efficiency observed between the thick (127 μm) and thin (25 μm) composite films could be attributed mainly to concentration effects.

Analysis of the UV–vis spectra of the AAP2-PDMS composite film was carried out in a manner similar to those of AAP1 based films. A similar trend was observed when the AAP2-PDMS composite film was irradiated with alternating UV and green lights. However, the spectra of the AAP2 showed an overlap of the absorbance of the *trans*-and-*cis* isomers which limits selective excitation resulting in less efficient isomerization (~83%)

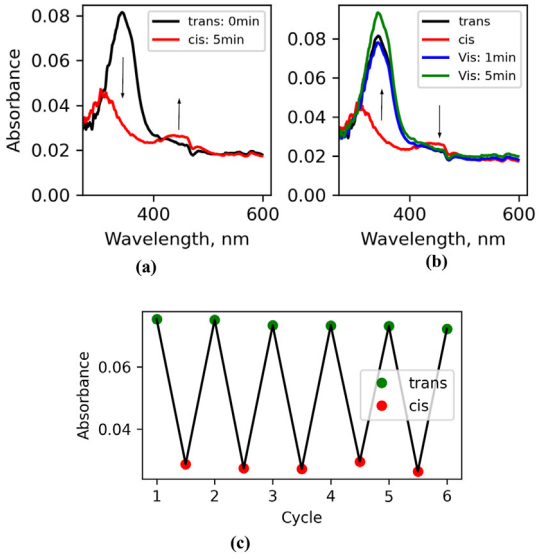

Fig. 6. UV–vis absorbance spectral changes of the hybrid thin film of the AAP1-PDMS composite film; (**a**) *trans*-to-*cis*-isomerization after continuous 5 min irradiation at λ = 365 nm; (**b**) spectra of a sample of the composite film (*cis*-to-*trans* isomerization) upon irradiation with λ = 525 nm at different times from 1 to 5 min. The rise in the base line of the spectra of the solid thin film is due to scattering of incident light. (**c**) Optical switching characteristics of the composite film upon alternating irradiation with UV and green light at 340 nm absorbance wavelength for four cycles. (For interpretation of the references to color in this figure legend, the reader is referred to the Web version of this article.)

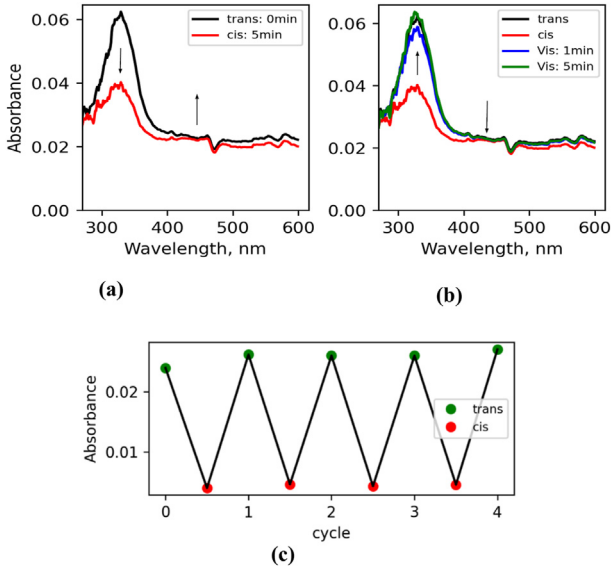

Fig. 7. UV–vis absorbance spectral changes of the hybrid thin film of the AAP2-PDMS composite film; (**a**) *trans*-to-*cis*-isomerization after continuous 5 min irradiation at λ = 365 nm; (**b**) spectra of a sample of the composite film (*cis*-to-*trans* isomerization) upon irradiation with λ = 525 nm at different times from 1 to 5 min. The rise in the base line of the spectra of the solid thin film is due to scattering of incident light. (**c**) Optical switching characteristics of the composite film upon alternating irradiation with UV and green light at 340 nm absorbance wavelength for four cycles. (For interpretation of the references to color in this figure legend, the reader is referred to the Web version of this article.)

of the AAP2 Embedded in the solid state PDMS composite films (Fig. 7a). This overlap could be due to some geometric constraints that result when the AAP2 photoswitch is doped into the PDMS matrix. A second irradiation with green light for 5 min results in the retrieval of the original spectrum with a slightly higher intensity of the peak at the 340 nm, indicating that a small percentage of the *cis*-form of the AAP2 was present in the of the original sample (Fig. 7b).

Although, our results show that the conversion efficiency of the AAP2 is generally lower compared to that of AAP1, its incomplete isomerization is far better than the extensively studied azobenzene counterpart. For example, the switching efficiency of azobenzene embedded in a polymer matrix (*Trans*-4-methacryloyloxyazobenzene) in hexane

was 71% [66,69]. This observation clearly indicates that the AAPs have more favorable photoswitching properties compared to those of azobenzenes a fact that has been

corroborated by previous reports on solution based studies of other AAP derivatives. In addition, the results in this study showed that the hydroxyl (AAP1) and carboxyl (AAP2) containing molecules gave different results after doping of PDMS with acetone solution of the AAPs at 150 °C. For comparison purposes, the band maxima and conversion efficiency are given in the Supporting Information (see Table S1). Similar to inorganic oxide based composites, the performance and strength of the hybrid organic-polymer films could be improved by incorporating additional fillers into the polymer matrix [54–56].

The morphology (Fig. 8) of the spin-coated AAP1-PDMS composite film was examined by Scanning Electron Microscope (SEM). The SEM images show that the morphology the AAP-PDMS composite films is uniformly regular with no presence of other discrepancy phases.

3.5. Photoinduced bending actuation

To test the actuation ability of the thin film, a 4.5 mm × 4.5 mm with 25 μm thickness was cut. Then, the reversible light driven deformation of the films was investigated by alternating illumination of UV and green light, respectively, and imaged under a microscope (Fig. 9). A schematic view of the experimental setup for the actuation measurement is shown in Fig. 9a. A sample of the AAP1-PDMS composite film is placed vertically on microscope platform. A section of the film is manually lifted off the glass to create a gap. Image of the AAP1-PDMA film is then captured first for the *trans* state and then after each UV and green light irradiation (Fig. 9b).

The image is then analyzed with Gwydion [70] software to measure the changes in width of the gap (See Fig. S3; and Table S2 in the Supporting Information). Upon irradiation with 365 nm UV light, the AAP-PDMS films bend away to a small extent from the glass slide.

by ~ 2.7 μm size change and return to the initial state when exposed to 525 nm green light. We presumed that at around 360 nm, most incident photons were absorbed by the embedded AAP units and the isomerization induced a stress in the films, and thereby led to a bending deformation of the whole systems. When the bent film was exposed to green light, *cis*-AAP went back to the original *trans*-state embedded within the PDMS matrix (see Fig. S3; in the Supporting Information). The repeatability of this behavior is confirmed over four cycles of actuation without loss of photoresponsive behavior (see Fig. S3 and Table S2 in the Supporting Information). This led us to hypothesize that the AAP-PDMS composite film described in this study could potentially function as a photodynamic system that change its size by photoinduced isomerization. In particular, the observed photostability of the AAP functionalized PDMS composite films opens a wide range of potential applications that include pure photonics and conformable devices.

4. Conclusion

In conclusion, we have successfully fabricated arylazopyrazole embedded polydimethylsiloxane composite films that display near quantitative (~100) reversible *trans*-to-cis photoisomerization in the solid-sate. These composite films are designed to illustrate the versatility and excellent performance of the arylazopyrazole based molecular switches. The composite films were prepared by directly embedding the arylazopyrazole photoswitches into the polydimethylsiloxane matrix. The transparent and flexible composite films were found to display an efficient reversible *trans*-to-*cis* isomerization of the arylazopyrazole photochromic units in the polydimethylsiloxane host matrix upon alternating irradiation with UV (λ = 365 nm) and green (λ= 525 nm) lights. In particular, the 6-cabon alkyl chain gave a composite film with remarkable reversible light-induced isomerization in the solid-state polymeric material. The UV–vis spectra of the solid-sate samples shows >98% conversion to the *cis*-isomer. This conversion efficiency (~100) is comparable to those of solution based samples for AAP and azobenzenes described in the literature. Furthermore, we demonstrated that upon exposure to alternating UV and green light the composite films showed a slight macroscopic reversible bending behavior to a smaller extent. These results imply that the arylazopyrazole domains embedded in the polydimethylsiloxane matrix can work as micro-actuators to afford macroscopic deformation of the whole film. The composite film also showed good recyclability under alternating treatment with light of specific

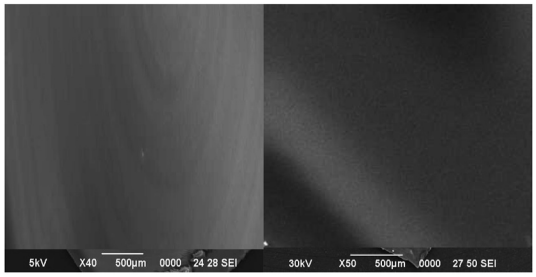

(a) (b)

Fig. 8. SEM images of the AAP1-PDMS composite film containing 0.020 M of the AAP1 photoswitch; (**a**) 5 kV, ×40 magnification and (**b**) 30 kV, ×50 magnification.

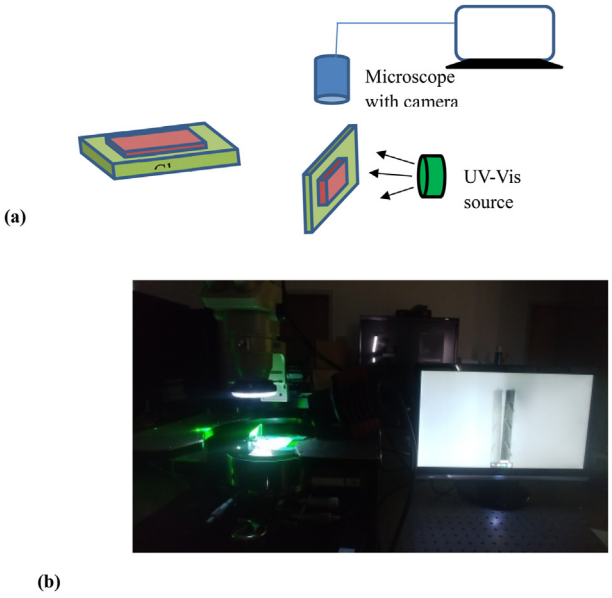

(a)

(b)

Fig. 9. (**a**) Schematics view of the experimental setup for the actuation measurements; (**b**) Optical Microscope setup with Camera and placement of the sample in a vertical position for UV and green light irradiation. (For interpretation of the references to color in this figure legend, the reader is referred to the Web version of this article.)

wavelengths up to four times, indicating a good optical switching performance and strong fatigue resistance. We postulate that the excellent reversible solid-state photoswitching of the arylazopyrazole doped composite films reported here may enable great potential applications for optoelectronic devices with tunable electronic and optical properties.

CRediT authorship contribution statement

Kesete Ghebreyessus: Conceptualization, Investigation, Supervision, Writing – review & editing. **Ikemefuna Uba:** Conceptualization, Investigation, Writing – original draft. **Demetris Geddis:** Conceptualization, Supervision. **Uwe Hömmerich:** Supervision, Validation.

Declaration of competing interest

The authors declare that they have no known competing financial interests or personal relationships that could have appeared to influence the work reported in this paper.

Acknowledgements

The work at Hampton University was supported through the Partnership for Research and Education in Materials (PREM) by U.S. National Science Foundation (NSF) (NSF PREM: Award # 1827820).

Appendix A. Supplementary data

Supplementary data to this article can be found online at https://doi.org/10.1016/j.jssc.2021.122519.

References

[1] X. Pang, J. Lv, C. Zhu, L. Qin, Y. Yu, Photodeformable azobenzene-containing liquid crystal polymers and soft actuators, Adv. Mater. 31 (2019), 1904224, https://doi.org/10.1002/adma.201904224.
[2] T. Taniguchi, T. Asahi, H. Koshima, Photomechanical azobenzene crystals, Crystals 9 (2019) 437–521, https://doi.org/10.3390/cryst9090437.
[3] C. Lv, S.N. Varanakkottu, T. Baier, S. Hardt, Controlling the trajectories of nano/micro particles using light-actuated marangoni flow, Nano Lett. 18 (2018) 6924–6930, https://doi.org/10.1021/acs.nanolett.8b02814.
[4] X. Xiaa, H. Yua, L. Wanga, Z. Denga, K.J. Sheab, Z. Abdina, Preparation of redox-and-photo-responsive ferrocene-and-azobenzene-based polymers films and their properties, Eur. Polym. J. 100 (2018) 103–110, https://doi.org/10.1016/j.eurpolymj.2018.01.023.
[5] T. Mosciatti, S. Bonacchi, M. Gobbi, L. Ferlauto, F. Liscio, L. Giorgini, E. Orgiu, P. Samorì, Optical input/electrical output memory elements based on a liquid crystalline azobenzene polymer, ACS Appl. Mater. Interfaces 8 (2016) 6563–6569, https://doi.org/10.1021/acsami.5b12430.
[6] M. Morikawa, H. Yang, K. Ishiba, K. Masutani, J.K.-H. Hui, N. Kimizuka, A liquid arylazopyrazole derivative as molecular solar thermal fuel with long-term thermal stability, Chem. Lett. 49 (2020) 736–740, https://doi.org/10.1246/cl.200171.
[7] M.A. Gerkman, R.S.L. Gibson, J. Calbo, Y. Shi, M.J. Fuchter, G.G.D. Han, Arylazopyrazoles for long-term thermal energy storage and optically triggered heat release below 0 °C, J. Am. Chem. Soc. 142 (2020) 8688–8695, https://doi.org/10.1021/jacs.0c00374.
[8] J. Zhang, W. Ma, X.-P. He, H. Tan, Taking orders from light: photo-switchable working/inactive smart surfaces for protein and cell adhesion, ACS Appl. Mater. Interfaces 9 (2017) 8498–8507, https://doi.org/10.1021/acsami.6b15599.
[9] C. Zhong, M. Hu, U. Azhar, X. Chen, Y. Zhang, S. Zhang, C. Lu, Smart copolymer-functionalized flexible surfaces with photoswitchable wettability: from superhydrophobicity with "rose petal" effect to superhydrophilicity, ACS Appl. Mater. Interfaces 11 (2019) 25436–25444, https://doi.org/10.1021/acsami.9b07767.
[10] S.N. Varanakkottu, S.D. George, T. Baier, S. Hardt, M. Ewald, M. Biesalski, Particle manipulation based on optically controlled free surfaces, hydrodynamics, Angew. Chem. Int. Ed. 52 (2013 7291 7295), https://doi.org/10.1002/anie.201302111.
[11] W. Wiemann, R. Niebuhr, A. Juan, E. Cavatorta, B.J. Ravoo, P. Jonkheijm, Photo-responsive bioactive surfaces based on cucurbit[8]uril-mediated host–guest interactions of arylazopyrazoles, Chem. Eur J. 24 (2018) 813–817, https://doi.org/10.1002/chem.201705426.
[12] J. Karcher, Z.L. Pianowski, Photocontrol of drug release from supramolecular hydrogels with green light, Chem. Eur J. 245 (2018) 11605–11610, https://doi.org/10.1002/chem.201802205.
[13] P.R.A. Chivers, D.K. Smith, Spatially-resolved soft materials for controlled release – hybrid hydrogels combining a robust photo-activated polymer gel with an interactive supramolecular gel, Chem. Sci. 8 (2017) 7218–7227, https://doi.org/10.1039/C7SC02210G.
[14] J. Park, L.-B. Sun, Y.-P. Chen, Z. Perry, H.C. Zhou, Azobenzene-functionalized metal-organic polyhedra for the optically responsive capture and release of guest molecules, Angew. Chem. Int. Ed. 53 (2014) 5842–5846, https://doi.org/10.1002/anie.201310211.
[15] M.J. Clemente, R.M. Tejedor, P. Romero, J. Fitremann, L. Oriol, Photoresponsive supramolecular gels based on amphiphiles with azobenzene and maltose or polyethyleneglycol polar head, New J. Chem. 39 (2015) 4009–4019, https://doi.org/10.1039/C4NJ02012J.
[16] D. Bleger, J. Schwarz, A.M. Brouwer, S. Hecht, o-Fluoroazobenzenes as readily synthesized photoswitches offering nearly quantitative two-way isomerization with visible light, J. Am. Chem. Soc. 134 (2012) 20597–20600, https://doi.org/10.1021/ja310323y.
[17] S. Samanta, A.A. Beharry, O. Sadovski, T.M. McCormick, A. Babalhavaeji, V. Tropepe, G.A. Woolley, Photoswitching azo compounds in vivo with red light, J. Am. Soc. 134 (2013) 9777–9784, https://doi.org/10.1021/ja402220t.
[18] A.A. Beharry, O. Sadovski, G.A. Woolley, Azobenzene photoswitching without ultraviolet light, J. Am. Chem. Soc. 133 (2011) 19684–19687, https://doi.org/10.1021/ja209239m.
[19] A. Goulet-Hanssens, F. Eisenreich, S. Hecht, Enlightening materials with photoswitches, Adv. Mater. 32 (2020), 1905966, https://doi.org/10.1002/adma.201905966.
[20] C.E. Weston, R.D. Richardson, P.R. Haycock, A.J.P. White, M.J. Fuchter, Arylazopyrazoles: azoheteroarene photoswitches offering quantitative isomerization and long thermal half-lives, J. Am. Chem. Soc. 136 (2014) 11878–11881, https://doi.org/10.1021/ja505444d.
[21] R.S.L. Gibson, J. Calbo, M.J. Fuchter, Chemical $Z-E$ isomer switching of arylazopyrazoles using acid, ChemPhotoChem 3 (2019) 372–377, https://doi.org/10.1002/cptc.201900065.
[22] C.-W. Chu, B.J. Ravoo, Hierarchical supramolecular hydrogels: self-assembly by peptides and photo-controlled release via host–guest interaction, Chem. Commun. 53 (2017) 12450–12453, https://doi.org/10.1039/C7CC07859E.
[23] A. Sallee, K. Ghebreyessus, Photoresponsive Zn^{2+}-specific metallohydrogels coassembled from imidazole containing phenylalanine and arylazopyrazole derivatives, Dalton Trans. 49 (2020) 10441–10451, https://doi.org/10.1039/D0DT01809K.
[24] C.W. Chu, L. Stricker, T.M. Kirse, M. Hayduk, B.J. Ravoo, Light-Responsive Arylazopyrazole Gelators, From organic to aqueous media and from supramolecular to dynamic covalent chemistry, Chem. Eur J. 25 (2019) 6131–6140, https://doi.org/10.1002/chem.201806042.
[25] S. Lamping, L. Stricker, B.J. Ravoo, Responsive surface adhesion based on host–guest interaction of polymer brushes with cyclodextrins and arylazopyrazoles, Polym. Chem. 10 (2019) 683–690, https://doi.org/10.1039/C8PY01496E.
[26] M. Schnurbus, L. Stricker, B.J. Ravoo, B. Braunschweing, Smart air–water interfaces with arylazopyrazole surfactants and their role in photoresponsive aqueous foam, Langmuir 34 (2018) 6028–6035, https://doi.org/10.1021/acs.langmuir.8b00587.
[27] M. Schnurbus, R.A. Campbell, J. Droste, C. Honnigfort, D. Glikman, P. Gutfreund, M.R. Hansen, B. Braunschweig, Photo-switchable surfactants for responsive Air−Water interfaces: azo versus arylazopyrazole amphiphiles, J. Phys. Chem. B 124 (2020) 6913–6923, https://doi.org/10.1021/acs.jpcb.0c02848.
[28] S. Engel, N. Möller, L. Stricker, M. Peterlechner, B.J. Ravoo, Modular system for the design of stimuli-responsive multifunctional nanoparticle aggregates by use of host–guest chemistry, Small 14 (2018), 1704287, https://doi.org/10.1002/smll.201704287.
[29] N. Möller, T. Hellwig, L. Stricker, S. Engel, C. Fallnich, B.J. Ravoo, Near-infrared photoswitching of cyclodextrin–guest complexes using lanthanide-doped $LiYF_4$ upconversion nanoparticles, Chem. Commun. 53 (2017) 240–243, https://doi.org/10.1039/C6CC08321H.
[30] J. Moratz, L. Stricker, S. Engel, B.J. Ravoo, Controlling complex stability in photoresponsive macromolecular host–guest systems: toward reversible capture of DNA by cyclodextrin vesicles, Macromol. Rapid Commun. 39 (2018), 1700256, https://doi.org/10.1002/marc.201700256.
[31] C.E. Weston, A. Krämer, F. Colin, Ö. Yildiz, M.G.J. Baud, M.J. Fuchter, Toward photopharmacological antimicrobial chemotherapy using photoswitchable amidohydrolase inhibitors, ACS Infect. Dis. 3 (2017) 152–161, https://doi.org/10.1021/acsinfecdis.6b00148.
[32] V. Adam, D.K. Prusty, M. Centola, M. Škugor, J.F. Hannam, J. Valero, B. Klöckner, M. Famulok, Expanding the toolbox of photoswitches for DNA nanotechnology using arylazopyrazoles, Chem. Eur J. 24 (2018) 1062–1066, https://doi.org/10.1002/chem.201705500.
[33] I.H. Chen, Y. Zhao, Applications of light-responsive systems for cancer theranostics, ACS Appl. Mater. Interfaces 10 (2018) 21021–21034, https://doi.org/10.1021/acsami.8b01114.
[34] K. Ghebreyessu, S.M. Cooper Jr., Photoswitchable arylazopyrazole-based ruthenium(II) arene complexes, Organometallics 36 (2017) 3360–3370, https://doi.org/10.1021/acs.organomet.7b00493.
[35] W. Chen, R.H.W. Lam, J. Fu, Photolithographic surface micromachining of polydimethylsiloxane (PDMS), Lab Chip 12 (2012) 391–395, https://doi.org/10.1039/C1LC20721K.
[36] K.A. Heyries, C.A. Marquette, L.J. Blum, Straightforward protein immobilization on sylgard 184 PDMS microarray surface, Langmuir 23 (2007) 4523–4527, https://doi.org/10.1021/la070018o.
[37] A. Zahid, B. Dai, R. Hong, D. Zhang, Optical properties study of silicone polymer PDMS substrate surfaces modified by plasma treatment, Mater. Res. Express 4 (2017), 105301, https://doi.org/10.1088/2053-1591/aa8645.

[38] A. Mata, A.J. Fleischman, S. Roy, Characterization of polydimethylsiloxane (PDMS) properties for biomedical micro/nanosystems, Biomed. Microdevices 7 (2005) 281–293, https://doi.org/10.1007/s10544-005-6070-2.
[39] W.A. Bauer, M. Fischlechner, C. Abell, W.T.S. Huck, Hydrophilic PDMS microchannels for high-throughput formation of oil-in-water microdroplets and water-in-oil- in-water double emulsions, Lab Chip 10 (2010) 1814–1819, https://doi.org/10.1039/C004046K.
[40] A. Angelini, U. Agero, F.F. Lupi, M. Fretto, F. Pirri, F. Frascella, Real-time and reversible light-actuated microfluidic channel squeezing in dye-doped PDMS, Soft Matter 16 (2020) 4383–4388, https://doi.org/10.1039/D0SM00217H.
[41] S. Deguchi, J. Hotta, S. Yokoyama, T.S. Matsui, Viscoelastic and optical properties of four different PDMS polymers, J. Micromech. Microeng. 25 (2015), 097002, https://doi.org/10.1088/0960-1317/25/9/097002.
[42] Z. Zhao, J. Tian, Ultraviolet–visible/fluorescence behaviors of a spiropyran/polydimethylsiloxane composite film under acid vapors, J. Appl. Polym. Sci. 137 (2017), 45199, https://doi.org/10.1002/app.45199.
[43] Y.-S. Nama, I. Yoob, O. Yarimagac, I.S. Parka, D.-H. Parka, S. Song, J.-M. Kim, C.W. Lee, Photochromic spiropyran-embedded PDMS for highly sensitive and tunable optochemical gas sensing, Chem. Commun. 50 (2014) 4251–4254, https://doi.org/10.1039/C4CC00567H.
[44] E. Kizilkan, J. Strueben, A. Staubitz, S.N. Gorb, Bioinspired photocontrollable microstructured transport device, Sci Robot 2 (2017), https://doi.org/10.1126/scirobotics.aak9454 eaak9454.
[45] A. Gonzalez, E.S. Kengmana, M.V. Fonseca, G.G.D. Han, Solid-state photoswitching molecules: structural design for isomerization in condensed phase, Mater. Today Adv. 6 (2020), 100058, https://doi.org/10.1016/j.mtadv.2020.100058.
[46] S. Wankar, U.J. Pandit, I. Khan, Composite material derived via embedding ternary lanthanide complexes in inorganic/organic matrix, J. Lumin. 215 (2019), 116705, https://doi.org/10.1016/j.jlumin.2019.116705.
[47] Z.I. Pianowski, Recent implementations of molecular photoswitches into smart materials and biological systems, Chem. Eur J. 25 (2019) 5128–5144, https://doi.org/10.1002/chem.201805814.
[48] W.X. Que, Z. Sun, L.L. Wang, T. Chen, Photo-isomerization properties and heating-induced surface relief patterns from azobenzene-doped GeO2/gamma-glycidoxypropyltrimethoxy-silane organic-inorganic composite films, Opt Express 15 (2007) 6868–6873, https://doi.org/10.1364/OE.15.006868.
[49] M.V. Zdorovets, A.L. Kozlovskiy, D.I. Shlimas, D.B. Borgekov, Phase transformations in FeCo - Fe_2CoO_4/Co_3O_4-spinel nanostructures as a result of thermal annealing and their practical application, J. Mater. Sci. Mater. Electron. 32 (2021) 16694–16705, https://doi.org/10.1007/s10854-021-06226-5.
[50] A.L. Kozlovskiy, M.V. Zdorovets, Effect of doping of $Ce^{4+}/^{3+}$ on optical, strength and shielding properties of (0.5-x)TeO_2-0.25MoO-0.25Bi_2O_3-xCeO_2 glasses, Mater. Chem. Phys. 263 (2021), 124444, https://doi.org/10.1016/j.matchemphys.2021.124444.
[51] D.I. Tishkevich, S.S. Grabchikov, L.S. Tsybulskaya, V.S. Shendyukov, S.S. Perevoznikov, S.V. Trukhanov, E.L. Trukhanova, A.V. Trukhanov, D.A. Vinnik, Electrochemical deposition regimes and critical influence of organic additives on the structure of Bi films, J. Alloys Compd. 735 (2018) 1943–1948, https://doi.org/10.1016/j.jallcom.2017.11.329.
[52] D.I. Tishkevich, S.S. Grabchikov, S.B. Lastovskii, S.V. Trukhanov, T.I. Zubar, D.S. Vasin, A.V. Trukhanov, Correlation of the synthesis conditions and microstructure for Bi-based electron shields production, J. Alloys Compd. 749 (2018) 1036–1042, https://doi.org/10.1016/j.jallcom.2018.03.288.
[53] T. Zubar, V. Fedosyuk, D. Tishkevich, O. Kanafyev, K. Astapovich, A. Kozlovskiy, M. Zdorovets, D. Vinnik, S. Gudkova, E. Kaniukov, A.S.B. Sombra, D. Zhou, R.B. Jotania, C. Singh, S. Trukhanov, A. Trukhanov, The effect of heat treatment on the microstructure and mechanical properties of 2D nanostructured Au/NiFe system, Nanomater. Basel 10 (2020) 1077–1114, https://doi.org/10.3390/nano10061077.
[54] P.-J. Wang, D. Zhou, J. Li, L.-X. Pangc, W.-F. Liu, J.-Z. Su, C. Singh, S. Trukhanov, A. Trukhanov, Significantly enhanced electrostatic energy storage performance of P(VDF-HFP)/$BaTiO_3$-Bi(Li0.5Nb0.5)O_3 nanocomposites, Nano Energy 78 (2020), 105247, https://doi.org/10.1016/j.nanoen.2020.105247.
[55] A.L. Kozlovskiy, D.I. Shlimas, M.V. Zdorovets, Synthesis, structural properties and shielding efficiency of glasses based on TeO_2-(1-x)ZnO-xSm_2O_3, J. Mater. Sci. Mater. Electron. 32 (2021) 12111–12120, https://doi.org/10.1007/s10854-021-05839-0.
[56] A. Kozlovskiy, K. Egizbek, M.V. Zdorovets, M. Ibragimova, A. Shumskaya, A.A. Rogachev, Z.V. Ignatovich, K. Kadyrzhanov, Evaluation of the efficiency of detection and capture of manganese in aqueous solutions of FeCeOx nanocomposites doped with Nb_2O_5, Sensors 20 (2020) 4851, https://doi.org/10.3390/s20174851.</u>.
[57] S.V. Trukhanov, A.V. Trukhanov, V.G. Kostishin, L.V. Panina, I.S. Kazakevich, V.A. Turchenko, V.V. Oleinik, E.S. Yakovenko, L.Y. Matsui, Magnetic and absorbing properties of M-type substituted hexaferrites $BaFe_{12}$-x$GaxO_{19}$ (0.1 < x <1.2), J. Exp. Theor. Phys. 123 (2016) 461–469. https://doi.org/10.1134/S1063776116090089.
[58] A. Thakur, N. Sharma, M. Bhatti, M. Sharma, A.V. Trukhanov, S.V. Trukhanov, L.V. Panina, K.A. Astapovich, P. Thakur, Synthesis of barium ferrite nanoparticles using rhizome extract of Acorus Calamus: characterization and its efficacy against different plant phytopathogenic fungi, Nano-Struct. Nano-Objects 24 (2020), 100599, https://doi.org/10.1016/j.nanoso.2020.100599.
[59] T.I. Zubar, V.M. Fedosyuk, S.V. Trukhanov, D.I. Tishkevich, D. Michels, D. Lyakhov, A.V. Trukhanov, Method of surface energy investigation by lateral AFM: application to control growth mechanism of nanostructured NiFe films, Sci. Rep. 10 (2020), 14411, https://doi.org/10.1038/s41598-020-71416-w.
[60] S.V. Trukhanov, A.V. Trukhanov, H. Szymczak, Effect of magnetic fields on magnetic phase separation in anion-deficient manganite La0.70Sr0.30MnO_2.85, *Low Temp. Phys.* 37 (2011) 465–469, https://doi.org/10.1063/1.3614412.
[61] J.H. Park, S. Jang, D. Byun, J.K. Lee, Fluorine doped gallium tin oxide composite films as transparent conductive oxides on polyethylene terephthalate film prepared by electron cyclotron resonance metal organic chemical vapor deposition, Thin Solid Films 519 (2011) 6863–6867, https://doi.org/10.1016/j.tsf.2011.04.048.
[62] I. ul Haq, J. Jacob, K. Mehboob, K. Mahmood, A. Ali, N. Amin, S. Ikram, S. Hussain, Y. Feng, F. Ashraf, Effect of annealing temperature on the thermoelectric properties of ZnInO thin films grown by physical vapor deposition, *Phys. B Condens. Matter* 606 (2021), 412569, https://doi.org/10.1016/j.physb.2020.412569.
[63] K. Thongsuriwong, P. Amornpitoksuk, S. Suwanboon, Structure, morphology, photocatalytic and antibacterial activities of ZnO thin films prepared by sol–gel dip-coating method, Adv. Powder Technol. 24 (2013) 275–280, https://doi.org/10.1016/j.apt.2012.07.002.
[64] A.L. Kortekaas, J. Simke, D.W. Kurka, B.J. Ravoo, Rapid photoswitching of low molecular weight Arylazoisoxazole adhesives, ACS Appl. Mater. Interfaces 12 (2020) 32054–32060, https://doi.org/10.1021/acsami.0c03767.
[65] Z.-Y. Zhang, Y. He, Y. Zhou, C. Yu, L. Han, T. Li, Pyrazolylazophenyl ether-based photoswitches: facile synthesis, (Near-)Quantitative photoconversion, long thermal half-life, easy functionalization, and versatile applications in light-responsive systems, Chem. Eur J. 25 (2019) 13402–13410, https://doi.org/10.1002/chem.201902897.
[66] N.K. Joshi, M. Fuyuki, A.J. Wada, Polarity controlled reaction path and kinetics of thermal cis-to-trans isomerization of 4-aminoazobenzene, J. Phys. Chem. B 118 (2014) 1891–1899, https://doi.org/10.1021/jp4125205.
[67] S. Peng, Q. Guo, P.G. Hartley, T.C. Hughes, Azobenzene moiety variation directing self-assembly and photoresponsive behavior of azosurfactants, J. Mater. Chem. C 2 (2014) 8303–8312, https://doi.org/10.1039/C4TC00321G.
[68] G. Angelini, N. Canilho, M. Emo, M. Kingsley, C. Gasbarri, Role of solvent and effect of substituent on azobenzene isomerization by using room-temperature ionic liquids as reaction media, J. Org. Chem. 80 (2015) 7430–7434, https://doi.org/10.1021/acs.joc.5b00898.
[69] M. Moniruzzaman, J.D.R. Talbot, C.J. Sabey, G.F. Fernando, The use of ^{1}H NMR and UV–vis measurements for quantitative determination of trans/cis isomerization of a photo-responsive monomer and its copolymer, J. Appl. Polym. Sci. 100 (2006) 1103–1112, https://doi.org/10.1002/app.23490.
[70] D.N. Klapetek, P. Gwyddion, An open-source software for SPM data analysis, Cent. Eur. J. Phys. 10 (2012) 181–188, https://doi.org/10.2478/s11534-011-0096-2.